International Journal of Nano Science and Technology
Vol. 1, No. 3, April 2013, PP: 09 - 16
Available online www.ijnst.com

Research article

Zn_xCd_{1-x} (O) Thin Film Nanorods for PV Applications

Umer Mushtaq[1], Souad. A. Mohamad[2]

Department of Manufacturing and Materials. Kulliyah of Engineering
[1,2]International Islamic University, Malaysia
+60149708232, +60126772595

[1]mirkaz9@hotmail.com , [2]su3ad_albati@iium.edu.my

Abstract

Zn_xCd_{1-x} (O) nanorods (NRs) thin films were deposited on ITO glass substrate by using a single step controlled electrodeposition process. Thin films of crystalline nature with zinc and cadmium concentration changing from 10% - 90% were electrodeposited onto ITO conductive glass substrates. XRD analysis confirms a hexagonal wurtzite structure having grain size 37 nm. The FESEM images of Zn_xCd_{1-x} (O) shows that hexagonal nanorods were first time synthesized via electrodeposition technique at temperature of 90 ^oC and the size of each regular plane of hexagonal nanorods is about 63nm. The Cd content of $Zn_xCd_{1-x}O$ nanorods was as high as (about) 16.7 at% which as calculated by EDX. Remarkably, the ultra-violet (UV) near-band-edge (NBE) emission was red-shifted from 3.21 eV to 3.04 eV due to the direct modulation of band gap caused by Cd substitution, revealed by UV visible spectroscopy. Temperature is deemed as a key parameter for the formation of different morphologies of Zn_xCd_{1-x} (O) nanostructures. Finally, $Zn_xCd_{1-x}O$ hexagonal nanorods thin film is used as one electrode in photovoltaic cells to produce energy by absorbing the energy from the sun, this single junction cells have been put forward as a potential low-cost alternative to the widely used solar cells. However, the cost effectiveness is due to the $Zn_xCd_{1-x}O$ nanorods electrode.

Keywords: Electrodeposition, Zn_xCd_{1-x} (O), nanorods, thin films, band gap

1. Introduction

With ever increasing human population and improvement in the standard of living with time, energy production is one of the major concerns that human civilization will face over the next few decades. The most common and available forms of energy at present are the fossil fuels which are depleting quickly as the years are passing by. Consequently, many global organizations have already started looking for other alternatives. These alternatives must be; economical, sustainable and not degrade our environment.

One of the favorable materials for the production of optoelectronic devices, available in abundance is ZnO with advantages of low cost, non-toxicity and high chemical stability [1]. The wide band gap (3.37 eV), excellent c-axis orientation, good conductivity, piezoelectric behaviour and high-exciton binding energy (60 meV) that is much higher than other semiconductors materials, all of those makes it had excellent optoelectronic property [2]. Zinc oxide has proven its diverse usage in different fields of application which includes use in solar cells [3], photo catalysis [4,5], ultraviolet lasers [6], transparent electrodes [7], and gas sensors [8,9] etc. One of the well-known II – VI semiconductor with a direct band gap of 2.39 eV (563.6 nm) is Cadmium oxide (CdO) and it has found its use in various applications such as in solar cells, photodiodes [10], phototransistors[11] and sensors[12]. There are numerous reports on the synthesis of the ZnO through the usage of different methods including the Sol-Gel [13], self-assembly [14], chemical bath deposition [15], emulsion route [16], vapour phase transport [12], reactive sputter and spray pyrolysis techniques [17]. Also, some reports for the controlled potential electrodeposition and characterization of ZnTe thin films on indium tin oxides and structural characterization of electrodeposited zinc selenide thin films. [18, 19]

There are also several reported for the preparation of the CdO particles, but most of these methods only describe the thin film formation of CdO [20]. There is fairly little available literature on the synthesis of the particles as a free-standing powder. Recently, the formation of CdO films from Cd $(OH)_2$ films as a precursor has been described by Gujar et al in 2004 [21]. Field emission scanning electron microscope (FESEM) image, quantitative analysis and mapping were obtained by using JEOL JSM-6700F. For structural characterization, a high-resolution Shimadzu Lab XRD-6000 diffractometer in the θ-2θconfiguration with a copper anticathode (Cu Kα, 1.54 Å) has been used. Optical properties were monitored by transmittance using a xenon lamp in association with a 50 mm UV visible spectrometer.This study focuses on the synthesis of hexagonal $Zn_xCd_{1-x}O$ nanorods by varying the composition of the electrolyte and temperature of the electrolytic bath.

2. Materials and Method

The material selected as the substrate was Indium-Tin-Oxide (ITO). The ITO glass was cut into 2 cm x 2 cm by using a glass cutter. The chemical that were used in this experiment were Zinc Chloride ($ZnCl_2$), (Sigma Aldrich, ≥99.0%) and Cadmium Chloride ($CdCl_2$). They were used without further purification.The electrodeposition process consists of a two-electrode electrochemical cell and an electrolyte consists of different compositions of $ZnCl_2$ and $CdCl_2$ in various proportions. A glass coated with indium tin oxide (ITO) is used as a substrate and platinum was used as a counter electrode (CE). Conductive glass substrates were cleaned by rinsing with deionized water, acetone, followed by ultrasonic bath, dried and stored in vacuum. These conducting substrates were used as a working electrode (WE). A constant potential of -1.5 V was made constant by using a potentiostat. The variables controlled during the electrodeposition were deposition potential, temperature, deposition time and distance between the electrodes. The distance between WE and CE were fixed of 3.0 cm. After deposition, the films were rinsed with acetone and double distilled water.

3. Results and Discussion

3.1 FESEM Analysis

Controllable length of Zn_xCd_{1-x} (O) nanorods can be grown in solution by single step electrodeposition technique as seen in figure 1. The homogeneous nanorods with crystallized grains are formed at a relatively high temperature of 90 ^oC.

Figure 1a, b shows the low and high magnification FESEM images of Zn_xCd_{1-x} (O) nanorods grown on ITO glass substrate. The grown nanorods were highly dense, well aligned and having shapes of regular hexagon. The nanorods were about 50-100 nm in diameter and 4-5 μm in length. $ZnCl_2$ and $CdCl_2$ in the ratio of 3:2 concentrations were mixed in order to obtain hexagonal ZnCdO nanorods. Figure 1c-f shows FESEM images of ZnCdO films grown using 2:3 and 4:1 ratio of $ZnCl_2$ and $CdCl_2$ powder, respectively. It can be seen that the nanorods on the surface become less dense and random. Also with the increase in the concentration of $CdCl_2$, the amount of CdO on the surface increased.

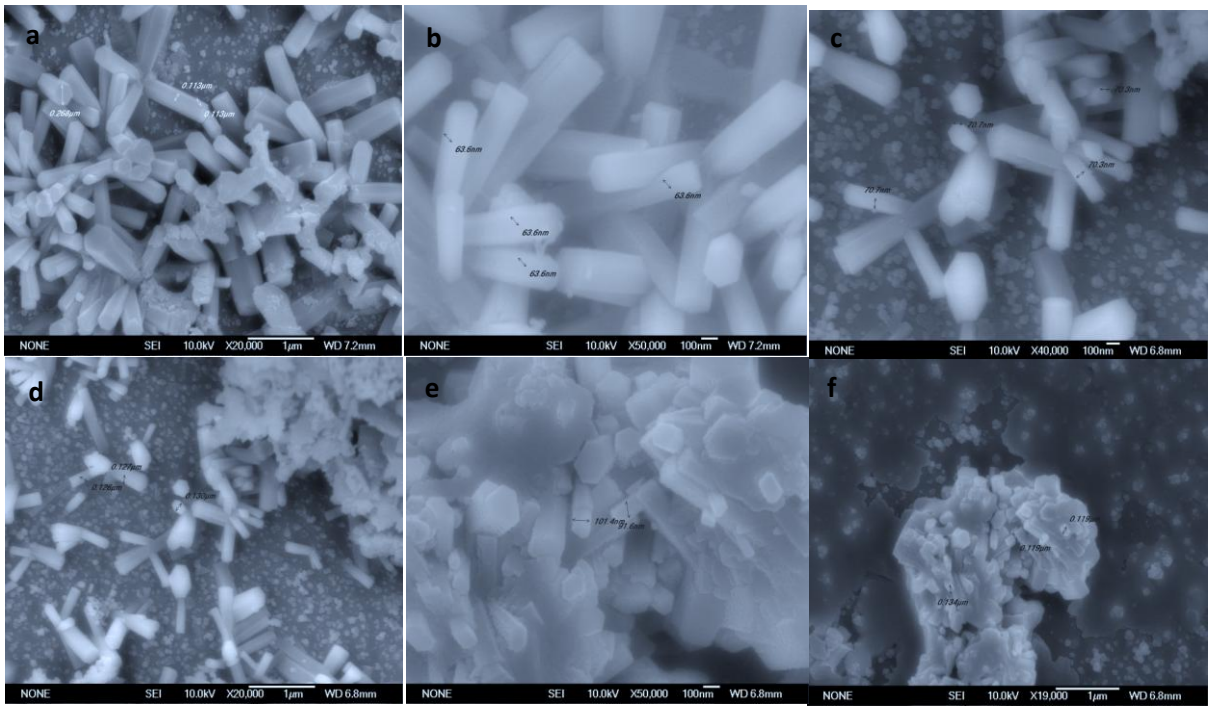

Fig. 1: FESEM images (top-view) of Zn_xCd_{1-x} (O) obtained from different compositions of $ZnCl_2$ and $CdCl_2$

3.2 Structural Characterization

The crystal structure of Zn_xCd_{1-x} (O) thin film nanorods was investigated through X-ray diffraction (XRD) as shown in figure 2. Figure 2 shows the XRD patterns of five samples with x varying from 10 – 90 % deposited at 90 ^oC. All the diffraction peaks in the patterns correspond to the reflection of wurtzite-structured ZnO planes and the samples $Zn_{0.2}Cd_{0.8}$ (O), $Zn_{0.4}Cd_{0.6}$ (O) and $Zn_{0.5}Cd_{0.5}$ (O) have a strong (002) peak along with (100) and (101) peaks but in $Zn_{0.6}Cd_{0.4}$ (O) and $Zn_{0.8}Cd_{0.2}$ (O) the intensity of (101) peak is more than the (002) peak. This suggests that all the prepared ZnO thin films have a hexagonal wurtzite structure and are preferentially oriented along the c-axis perpendicular to the substrate surface. The presence of prominent peaks shows that films are polycrystalline in nature. As-grown $Zn_xCd_{1-x}O$ NRs showed major XRD peaks at 2θ of 38.25^o and 31.75^o that can be indexed to reflections from (200) and (101) planes of hexagonal ZnO, respectively, according to the JCPDS no. 36-1451. The additional peaks from (111) and (311) planes corresponding to cubic CdO (JCPDS no. 05-0640) besides hexagonal peaks of ZnO.

In order to make further analysis of the influence of deposition temperature to the crystallization, the crystallite size of the thin film can be calculated according to Scherrer equation as given below:

$$D = \frac{0.9\,\lambda}{FWHM\ Cos\theta}$$

where 0.9 is a constant, θ is the diffraction angle, λ (= 1.54059 Å) is the wavelength of X-ray used, and FWHM is the full width at half maximum.

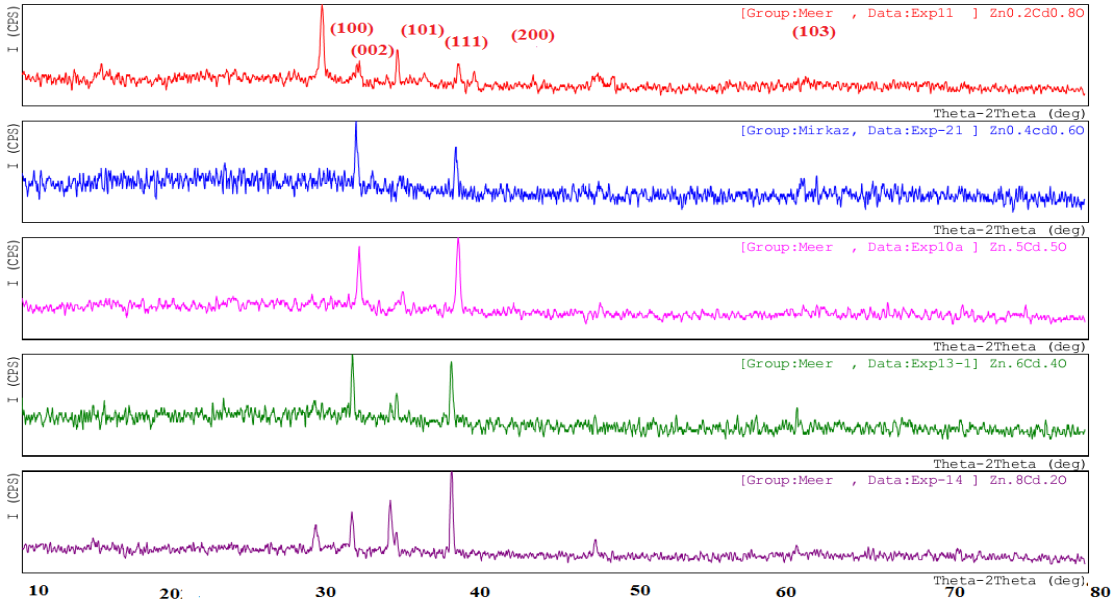

Fig. 2: XRD Patterns of $Zn_xCd_{1-x}O$ thin films on glass substrate deposited at 90 ^oC

3.3 UV Visible Spectroscopy

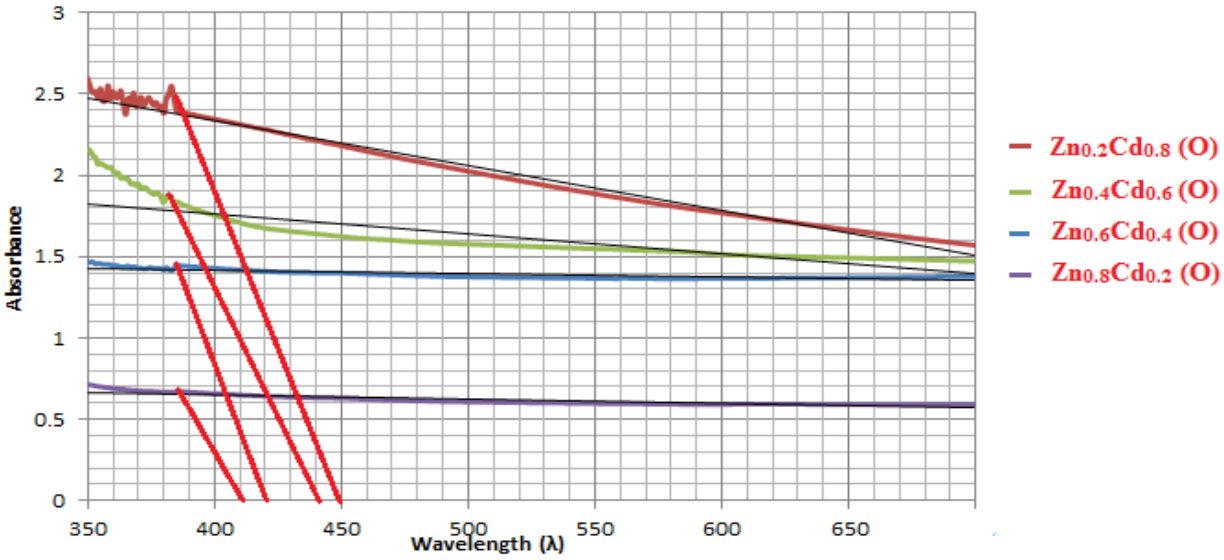

Fig.3: UV visible of Zn_xCd_{1-x} (O) thin films grown at 90 ^oC

The absorbance spectra of the samples taken using UV-Vis spectrometer show the interference fringes which has its origin in the interference of light reflected between air-film and film-substrate interface. The variation of $(\alpha h\nu)^2$ versus λ were plotted in figure 4. The energy band gap E_g of the samples is evaluated from the intercept of the linear portion of the each curve for samples with different solvents with (λ) on x-axis. The optical gap of the samples was found to vary from 2.75-3.02 eV for the differently synthesized samples depending on the amount of cadmium concentration. The UV visible of different film samples and show the effect of different composition of cadmium content on the band gap of ZnO which changes from 3.3 eV to 2.75 eV. The addition of Cd tailors the band gap of the ZnO and produces a red shift of the absorption of the alloy semiconductor films proportional to the cadmium content. These results indicate the use of different composition during the precursor formation will finally affects the surface morphology, crystal structure and finally the photonic properties relevant to their applications as transparent conductor in various solid state devices.

3.4 PV Characterisation

The current–voltage characteristics of the devices were measured with a digital source meter (Keithley KPCI-488LA, computer-controlled) under one sun AM-1.5G irradiation from a solar simulator. The spectra of the efficiency of conversion of incident photons to current (IPCE) of the corresponding devices were recorded with a system comprising a Xe lamp, a monochromator and a source meter. The intensity of the Xenon lamp was 100mW/cm^2. Fig 5 and 6 shows the optimized J–V characteristic curve of the solar cell fabricated using the electrodeposited $Zn_{0.6}Cd_{0.4}$ (O) as working electrode and PEO + chitosan thin film as counter electrode. The results obtained from J-V characterisation of Zn_xCd_{1-x} (O)/PEO +Chitosan cells is tabulated in table 1. It can be seen in table 1 that the V_{oc} under light ranges from 160 mV to 490 mV depending on cadmium doping. For the optimized solar cell the light conversion efficiency obtained is 1.6% with a fill factor of 34.2 %.

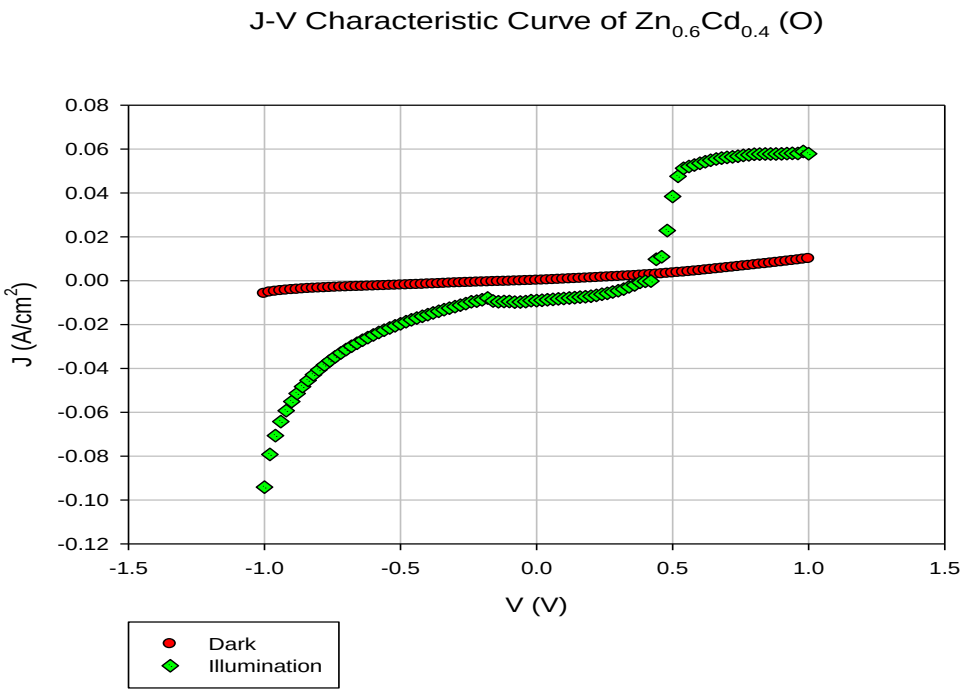

Fig 4: Diode like I-V characteristic curve of $Zn_{0.6}Cd_{0.4}$ (O)/PEO + Chitosan in the dark and under illumination condition

International Journal of Nano Science and Technology
Vol. 1, No. 3, April 2013, PP: 09 - 16
Available online www.ijnst.com

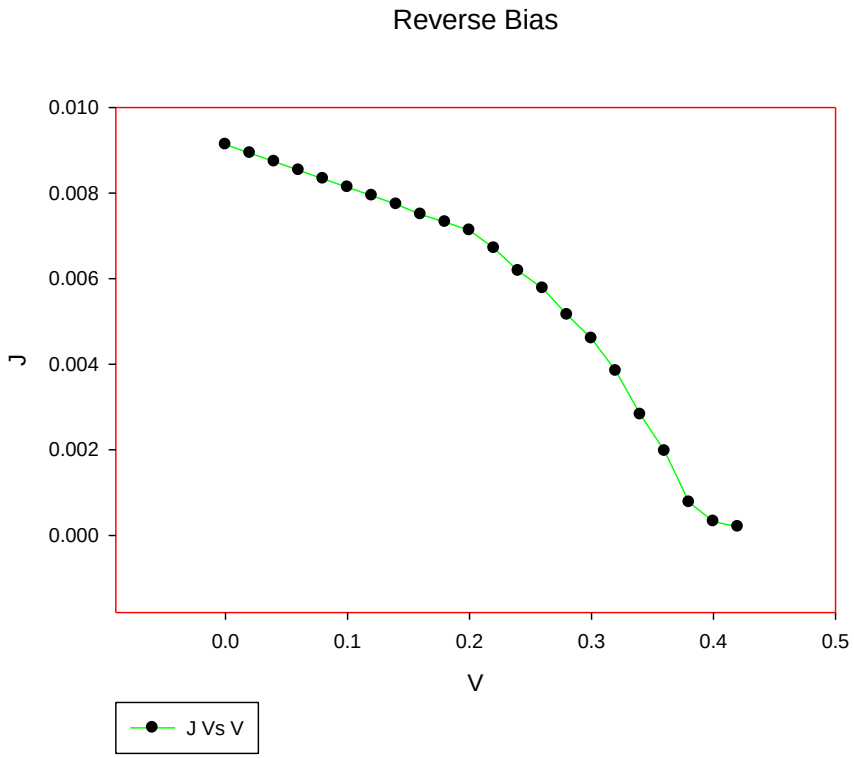

Fig 5: Reverse Bias for I-V characterisation of $Zn_{0.6}Cd_{0.4}$ (O)/PEO + Chitosan under illumination condition

Table 1: Open-circuit Voltage (Voc), Short-circuit Current (Isc), Fill factor (FF), maximum power point (υ) and efficiency (η) of the PV Cells fabricated

PV Cell	V_{oc}(mV)	J_{sc}(mA)	FF	H
	Light	Light		
Zn_1Cd_0 (O)/PEO + Chitosan	160	2.9	51.7%	0.24%
$Zn_0Cd_{1.0}$ (O)/PEO + Chitosan	240	0.95	30%	0.072%
$Zn_{0.6}Cd_{0.4}$ (O)/PEO + Chitosan	490	10	34.2%	1.6%
$Zn_{0.5}Cd_{0.5}$ (O)/PEO + Chitosan	260	2.4	54.4%	0.36%
$Zn_{0.4}Cd_{0.6}$ (O)/PEO + Chitosan	180	0.9	43.2%	0.7%

Conclusion

Electrodeposition technique was used to synthesize nanostructured electrodes of $Zn_xCd_{1-x}(O)$ on ITO glass substrate with several values of x in an aqueous medium containing Zn^{2+} and Cd^{2+} species for photovoltaic cell. The XRD studies confirmed that the thin films were polycrystalline and cubic (111) or hexagonal (002) oriented located at 32.03^o and the grain size of the film is 57.2 nm using Scherer's equation. The UV visible shows the band gap is altered by adding cadmium content and ranges from 2.75 -3.02 eV depending on the amount of cadmium concentration. Also, from the surface morphology it is seen that hexagonal nanorods of $Zn_xCd_{1-x}(O)$ were formed. The photovoltaic properties of $Zn_xCd_{1-x}(O)$ nanorods were obtained by using PEO + Chitosan as a counter electrode. The J-V characteristic curve of an optimised cell shows that the efficiency of 1.6% was achieved.

References

[1] L. Chen, Z. Ye, D. Ma, B. Zhao, C. Lin, L. Zhu, *J. Crystal Growth 283* (2005) 373.

[2] Dong Xin, Liu Dali, Yan Xiaonong, "The influence of annealing to ZnO thin films", Chinese *Journal of Luminescence, 26(4),* (2005) 535-537.

[3] Lokhande.B.J, P. U. "Studies on structural, optical and electrical properties of boron doped zinc oxide films prepared by spray pyrolysis technique", *Physica B,* 302, (2001) 59-63.

[4] Cheng Jingquan, Y. H. "Preparations and Applications of Ultrofine Zinc Oxide Powders", *Journal of Hebei Normal University(Natural Science), 24(4),* (2000), 509-512.

[5] Boule, C. R. "Oxidizing Species Involved in Photocatalytic Transformation on Zinc Oxide", *J. Photochem Photobiol.A: Chem,60* , (1991), 235.

[6] Singh.R.K, C. A. "Ultraviolet-assisted pulsed laser deposition of thin oxide flms", *Applied Surface Science 168* (2000), 239-243.

[7] Caglar Yasemin, Z. M. "Influence of the indium incorporation on the structural and electrical properties of zinc oxide films", *J. Optoelec and Advanc. Mat, 8(5),* (2006) 1867-1873.

[8] Shishiyanu.S, L. M. "Nanostructured zinc oxide gas sensors by successive ionic layer adsorption and reaction method and rapid photo thermal processing", *Thin Solid Films 488,* (2007)

[9] Mitra.P, C. A. "ZnO thin film Sensor", *Mater. Lett. 35,* (1998) 33-38.

[10] Henari, D. A. "Optical characterization of thermally evaporated thin CdO films", *Cryst. Res. Technol. 38(11),* (2003) 979-985.

[11] Carballeda-Galicia. D.M, C.P. J.S.S.D.R. "High transmittance CdO thin films obtained by the sol-gel method", *Electron Lett., 20,* (2000) 105-108.

[12] Ligang Yu, G. Z. "Fabrication of arrays of zinc oxide nanorods and nanotubes in aqueous solution under an external voltage", *Journal of Crystal Growth 299*, (2007) 184-188.

[13] Trinchi .A, L. W. "Investigation of sol–gel prepared Ga–Zn oxide thin", Sens Actuators A 108, (2003) 263-270.

[14] Ali.H.A, I. A. "Properties of self-assembled ZnO nanostructures", *Solid State Electron 46*, (2002) 1639-1642.

[15] Sivapunniyam Aarthy, W. N. "High-performance liquefied petroleum gas sensing based on nanostructures of zinc oxide and zinc stannate", *Sens and Actuators B: Chem* (2011)

[16] Sharmaa Bhupendra K, G. A. "Synthesis and characterization of polyaniline ZnO composite and its dielectric behavior", *Symthetic Materials 159*, (2009) 391-395.

[17] Rokn-Abadi, K.A "Enhancement of drift mobility of zinc oxide transparent-conducting films by a hydrogenation process", *Thin Solid Films 382,* (2001) 230

[18] S.A.Mohamad, B. I. "Contolled Potential Electrodeposition and Characterisation of ZnTe thin films on Indium Tin Oxide", *Advanced Material Research Vol 264-265,* (2011) 726-731.

[19] S.A. Mohamad, B. I. "Structure and Characterisation of Electrodeposited ZnSe Thin Film", *Advanced Material Research Vol 264-265* , (2011) 732-737.

[20] Ma. D, Y. W. "Deposition and characteristics of CdO films with absolutely", *Mater Lett 58*, (2003) 128-131.

[21] Gujar.T.P, S. W.-Y.-D.S. "Formation of CdO films from chemically deposited $Cd(OH)_2$ films as a precursor", *Applied Surface Science, 254*, (2008) 3813-3818